

Orthogonal Spin Arrangement in Quasi-Two-Dimensional $\text{La}_2\text{Co}_2\text{O}_3\text{Se}_2$

Yayoi Fuwa,[†] Takashi Endo,[†] Makoto Wakeshima,^{*,†} Yukio Hinatsu,[†] and Kenji Ohoyama[‡]

Division of Chemistry, Graduate School of Science, Hokkaido University, Sapporo 060-0810, Japan, and Institute for Materials Research, Tohoku University, Sendai 980-8577, Japan

Received October 6, 2010; E-mail: wake@sci.hokudai.ac.jp

Abstract: The crystal, electronic, and magnetic structures of the cobalt oxyselenide $\text{La}_2\text{Co}_2\text{O}_3\text{Se}_2$ were investigated through powder neutron diffraction measurements and band structure calculations. This oxyselenide crystallizes in a tetragonal layered structure with space group $I4/mmm$. The Co ion is sixfold-coordinated by two oxide ions and four selenide ions, and the face-sharing CoO_2Se_4 octahedra form Co_2OSe_2 layers. The band structure calculations revealed that the Co ion is in the divalent high-spin state. Rietveld analysis of the neutron diffraction profiles below 200 K demonstrated that the Co moments have a noncollinear antiferromagnetic structure with the propagation vector $\mathbf{k} = (\frac{1}{2}, \frac{1}{2}, 0)$. The ordered magnetic moment was determined to be $3.5\mu_B$ at 10 K, and the directions of the nearest-neighbor Co moments are orthogonal each other in the c plane.

Transition-metal oxychalcogenides and oxypnictides often crystallize in a two-dimensional (2D) structure due to anion site orderings because of the very different sizes of the oxide and chalcogenide/pnictide ions.¹ Recently, high-temperature superconductivity was discovered in layered iron oxypnictides.^{2–4} In such iron-based compounds, the 3d electrons of iron play a key role in the electrical and magnetic properties. For layered oxychalcogenides with strongly correlated electrons, the physical properties of several compounds have been investigated.^{5–9} The crystal structures and magnetic properties of $\text{La}_2\text{Fe}_2\text{O}_3\text{X}_2$ ($\text{X} = \text{S}, \text{Se}$) were reported by Mayer et al.¹⁰ For the isostructural compounds $\text{A}_2\text{Fe}_2\text{OX}_2\text{Q}_2$ ($\text{A} = \text{La}, \text{Nd}$ and $\text{Q} = \text{O}$; $\text{A} = \text{Sr}, \text{Ba}$ and $\text{Q} = \text{F}$), the Fe_2OX_2 monolayers and the A_2Q_2 bilayers are stacked along the c axis and the Fe_2OX_2 monolayers represent a frustrated antiferromagnetic checkerboard lattice.^{11–14}

Recently, the crystal and electronic structures and magnetic properties of a new cobalt oxyselenide, $\text{La}_2\text{Co}_2\text{O}_3\text{Se}_2$, have been studied by a few groups.^{15–17} Wang et al. reported that the Co ion is in the low-spin state and that $\text{La}_2\text{Co}_2\text{O}_3\text{Se}_2$ has a checkerboard spin lattice.¹⁵ On the other hand, the electronic structure calculated by Wu¹⁶ and our experimental results¹⁷ revealed that the Co ion is in the divalent high-spin state. To resolve this inconsistency, in the present work we have investigated the electronic and magnetic structures through powder neutron diffraction measurements and band structure calculations.

Powder samples of $\text{La}_2\text{Co}_2\text{O}_3\text{Se}_2$ were prepared through a solid-state reaction process as described elsewhere.¹⁷ The powder neutron diffraction measurements were carried out below 300 K in the range $3^\circ \leq 2\theta \leq 153^\circ$ at intervals of 0.1° using a wavelength of 1.8449 \AA . Measurements were performed on the Kinken powder diffractometer for high efficiency and high resolution measurements

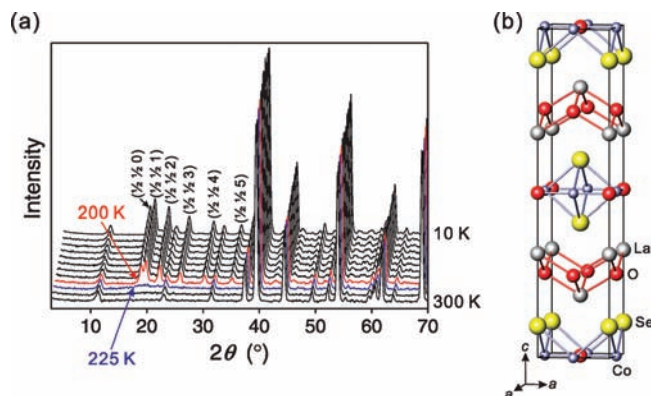


Figure 1. (a) Neutron diffraction profiles for $\text{La}_2\text{Co}_2\text{O}_3\text{Se}_2$ at 10, 30, 50, 75, 100, 125, 150, 175, 200, 225, 250, and 300 K. (b) Crystal structure of $\text{La}_2\text{Co}_2\text{O}_3\text{Se}_2$.

(HERMES) of the Institute for Materials Research (IMR) at Tohoku University,¹⁸ which was installed at the JRR-3 M Reactor of the Japan Atomic Energy Agency (JAEA), Tokai. The crystal and magnetic structures were determined by the Rietveld method using the FullProf suite.¹⁹ Calculations of the electronic structure and the density of states (DOS) were performed using the WIEN2k program package.²⁰ This program employs the full-potential linearized augmented plane wave + local orbitals (FP-LAPW+lo) method based on density functional theory (DFT). We used the generalized gradient approximation (GGA) + Hubbard U parameter for the Co 3d electrons.

Figure 1a shows the neutron diffraction profiles of $\text{La}_2\text{Co}_2\text{O}_3\text{Se}_2$ over the temperature range between 10 and 300 K. Only the nuclear Bragg reflections were observed at 300 K, and the crystal structure was refined by the Rietveld method. The obtained parameters are in good agreement with the parameters previously obtained from X-ray diffraction measurements. The structural parameters at 300 K are summarized in Table S1 in the Supporting Information. Figure 1b illustrates the crystal structure of $\text{La}_2\text{Co}_2\text{O}_3\text{Se}_2$. The Co ion is sixfold-coordinated by two oxide ions and four selenide ions, forming a CoO_2Se_4 octahedron, and the La ion is eightfold-coordinated by four oxide ions and four selenide ions. The Co_2OSe_2 monolayers consisting of face-sharing CoO_2Se_4 octahedra and the bilayers consisting of edge- and face-sharing LaO_4Se_4 decahedra are stacked along the c axis.

Figure 2a displays the total DOS and the partial DOS of Co for $\text{La}_2\text{Co}_2\text{O}_3\text{Se}_2$ obtained from the GGA + U calculations. The values of U and J_H for a Hubbard-like effective potential were set to be 5.0 and 0.9 eV, respectively.¹⁵ The occupied and unoccupied bands form a band gap of ~ 1.5 eV around the Fermi level. This result from the GGA + U calculations demonstrates that the Co ions are in the divalent state with the high-spin configuration and have a magnetic moment of $2.70\mu_B$. Figure 2b shows the Co 3d DOS. The energy levels of the unoccupied orbitals (d_{xz} , d_{xy} , $d_{3z^2-r^2}$) of

[†] Hokkaido University.

[‡] Tohoku University.

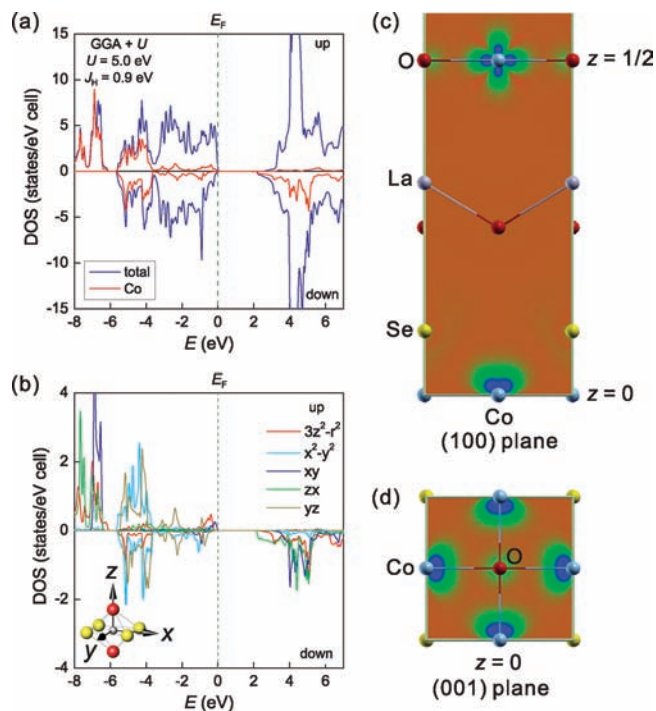


Figure 2. (a) Total density of states (DOS) and partial DOS of Co for $\text{La}_2\text{Co}_2\text{O}_3\text{Se}_2$ with $U = 5.0$ eV and $J_H = 0.9$ eV. (b) Partial DOS of the Co 3d orbitals. The Co–O bond axis is defined to be the z axis. (c) Spin density distribution in the (100) plane. (d) Spin density distribution in the (001) plane.

the Co ion are located at 3–5 eV, which indicates that the high-spin Co^{2+} state in the CoO_2Se_4 octahedron has one t_{2g} hole on the d_{zx} orbital and two e_g holes on the $d_{3z^2-r^2}$ and d_{xy} orbitals. These features of the total and partial DOS are similar to the previously reported ones.¹⁶ The spin density distribution mirrors the unoccupied orbitals. Figure 2c,d illustrates the spin density distribution. The spins of the Co ion exist along the c axis and along the Co–O bond axis. Because there is no magnetic interaction path along the c axis, it is suggested that the superexchange interaction via the Co–O–Co path play a key role in the magnetic interactions in the Co–O–Se layer.

In Figure 1a, a very broad peak was observed around $2\theta \approx 20^\circ$ below 250 K, and several Bragg reflections appear abruptly at 200 K. The temperature dependence of the magnetic susceptibility of $\text{La}_2\text{Co}_2\text{O}_3\text{Se}_2$ has a broad maximum around 250 K, and the specific heat shows a long-range antiferromagnetic ordering at 217 K.^{15,17} It is considered that a broad peak at 225–250 K and additional Bragg reflections below 200 K are attributable to magnetic diffuse scattering of short-range orderings in Co–O–Se layers and long-range ordering of the Co ions, respectively. The magnetic Bragg reflections are indexed to the $(\frac{1}{2} \frac{1}{2} l)$ planes, which indicates that the propagation vector \mathbf{k} in the magnetic ordered state is $\mathbf{k} = (\frac{1}{2}, \frac{1}{2}, 0)$. The symmetry and directions of the magnetic moments compatible with the crystal symmetry ($I4/mmm$) were obtained using the program SARA h .²¹ For the Co^{2+} ions on the $4c$ site, the decomposition of magnetic representation is

$$\Gamma = 0\Gamma_1^{(1)} + 2\Gamma_2^{(1)} + 0\Gamma_3^{(1)} + 1\Gamma_4^{(1)} + 0\Gamma_5^{(1)} + 1\Gamma_6^{(1)} + 0\Gamma_7^{(1)} + 2\Gamma_8^{(1)}$$

The constraint from the Landau theory requires four possible magnetic structures: the representations Γ_2 , Γ_4 , Γ_6 , and Γ_8 . The directions of the nearest-neighbor magnetic moments for the

Table 1. Basis Functions of the Irreducible Group Representation of the Space Group $I4/mmm$ Appearing in the Magnetic Representation with $\mathbf{k} = (\frac{1}{2}, \frac{1}{2}, 0)$

basis vector	atom 1 ^a			atom 2 ^a		
	m_x	m_y	m_z	m_x	m_y	m_z
Γ_2	Ψ_1	4	0	0	0	4
	Ψ_2	0	4	0	4	0
Γ_4	Ψ_3	0	0	4	0	4
Γ_6	Ψ_4	0	0	4	0	−4
Γ_8	Ψ_5	4	0	0	−4	0
	Ψ_6	0	4	0	−4	0

^a The atoms of the nonprimitive basis are defined as $(\frac{1}{2}, 0, 0)$ for 1 and $(0, \frac{1}{2}, 0)$ for 2.

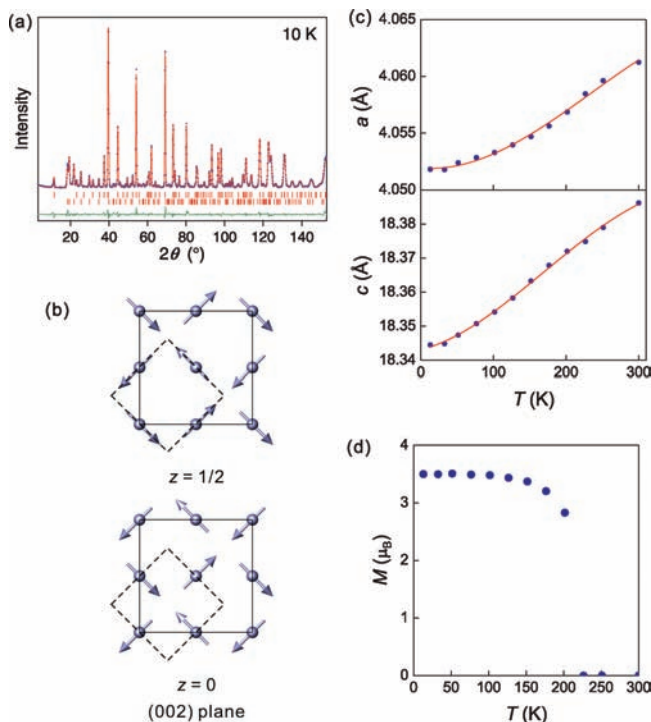


Figure 3. (a) Neutron diffraction profiles for $\text{La}_2\text{Co}_2\text{O}_3\text{Se}_2$ at 10 K. The calculated and observed diffraction profiles are shown as the top solid line and the \blacksquare markers, respectively. The upper set of vertical markers in the middle show positions calculated from nuclear Bragg reflections. The lower set of vertical markers in the middle show positions calculated from magnetic Bragg reflections. The trace at the bottom is a plot of the difference between the calculated and observed intensities. (b) Possible magnetic structure model of the Co moments. Broken lines represent the nuclear unit cell ($a \times a$), and solid lines represent the magnetic unit cell ($\sqrt{2}a \times \sqrt{2}a$). (c) Temperature dependence of the lattice parameters a and c . (d) Temperature dependence of the ordered magnetic moment of the Co ion.

representations Γ_2 and Γ_8 are orthogonal to each other in the c plane, while those for Γ_4 and Γ_6 lie on the c axis. The basis vectors for these representations are given in Table 1. The best fit was achieved using a model including only the representation Γ_8 . Figure 3a,b shows the profile refinement at 10 K and a possible magnetic structure model, respectively. The refined crystallographic and magnetic parameters at 10 K are summarized in Table S1. The magnetic moment was refined to be $3.53(1) \mu_B$ per Co^{2+} ion. This value is larger than the theoretical moment ($2.70 \mu_B$) obtained from the GGA + U calculation. This difference should be attributed to unquenched orbital moments.

The symmetry of the crystal structure was unchanged below 300 K. Figure 3c shows the temperature dependence of the lattice parameters. Both a and c increase monotonically with temperature. The Co–O and Co–Se bond lengths also increase monotonically.

These results suggest that magnetoelastic coupling and magnetostriction do not occur because of the long-range magnetic ordering of the Co ion.

Figure 3d shows the variation of the ordered magnetic moment. The ordered moment, which appears at 200 K, rapidly increases with decreasing temperature and becomes saturated below 100 K. A similar temperature dependence of the Co^{2+} moment was also shown to exist in other two-dimensional oxysulfides,²² which should be attributable to Ising-like anisotropy of the Co^{2+} ions.¹⁷

In summary, we have investigated the electronic and magnetic structures of the cobalt oxyselenide $\text{La}_2\text{Co}_2\text{O}_3\text{Se}_2$ with the layered structure. The magnetic ground state of the Co ions is a high-spin, noncollinear antiferromagnetically ordered state with the propagation vector $\mathbf{k} = (\frac{1}{2}, \frac{1}{2}, 0)$. The directions of the nearest-neighbor Co moments are orthogonal to each other in the c plane.

Acknowledgment. This work was supported in part by the Global COE Program (Project B01: Catalysis as the Basis for Innovation in Materials Science) from the Ministry of Education, Culture, Sports, Science, and Technology (MEXT), Japan.

Supporting Information Available: Table of structural parameters of $\text{La}_2\text{Co}_2\text{O}_3\text{Se}_2$ and crystallographic data in CIF format. This material is available free of charge via the Internet at <http://pubs.acs.org>.

References

- (1) Clarke, S. J.; Adamson, P.; Herkelrath, S. J. C.; Rutt, O. J.; Parker, D. R.; Pitcher, M. J.; Smura, C. F. *Inorg. Chem.* **2008**, *47*, 8473–8486.
- (2) Kamihara, Y.; Watanabe, T.; Hirano, M.; Hosono, H. *J. Am. Chem. Soc.* **2008**, *130*, 3296–3297.
- (3) Takahashi, H.; Igawa, K.; Arii, K.; Kamihara, Y.; Hirano, M.; Hosono, H. *Nature* **2008**, *453*, 376–378.
- (4) Ishida, K.; Nakai, Y.; Hosono, H. *J. Phys. Soc. Jpn.* **2009**, *78*, 062001.
- (5) Zhu, W. J.; Hor, P. H.; Jacobson, A. J.; Crisci, G.; Albright, T. A.; Wang, S. H.; Vogt, T. *J. Am. Chem. Soc.* **1997**, *119*, 12398–12399.
- (6) Kamihara, Y.; Matoba, M.; Kyomen, T.; Itoh, M. *J. Appl. Phys.* **2002**, *91*, 8864–8866.
- (7) Ijjaali, I.; Mitchell, K.; Haynes, C. L.; McFarland, A. D.; Van Duyn, R. P.; Ibers, A. *J. Solid State Chem.* **2003**, *176*, 170–174.
- (8) Indris, S.; Cabana, J.; Rutt, O. J.; Clarke, S. J.; Grey, C. P. *J. Am. Chem. Soc.* **2006**, *128*, 13354–13355.
- (9) Hyett, G.; Gál, Z. A.; Smura, C. F.; Clarke, S. J. *Chem. Mater.* **2008**, *20*, 559–566.
- (10) Mayer, J. M.; Schneemeyer, L. F.; Siegrist, T.; Waszczak, J. V.; Dover, B. V. *Angew. Chem., Int. Ed. Engl.* **1992**, *31*, 1645–1647.
- (11) Kabbour, H.; Janod, E.; Corraze, B.; Danot, M.; Lee, C.; Whangbo, M.-H.; Cario, L. *J. Am. Chem. Soc.* **2008**, *130*, 8261.
- (12) Fuwa, Y.; Wakeshima, M.; Hinatsu, Y. *J. Phys.: Condens. Matter* **2010**, *22*, 346003.
- (13) Zhu, J.-X.; Yu, R.; Wang, H.; Zhao, L. L.; Jones, M. D.; Dai, J.; Abrahams, E.; Morosan, E.; Fang, M.; Si, Q. *Phys. Rev. Lett.* **2010**, *104*, 216405.
- (14) Free, D. G.; Evans, J. S. *Phys. Rev. B* **2010**, *81*, 214433.
- (15) Wang, C.; Tan, M. Q.; Feng, C. M.; Ma, Z. F.; Jiang, S.; Xu, Z. A.; Cao, G. H.; Matsubayashi, K.; Uwatoko, Y. *J. Am. Chem. Soc.* **2010**, *132*, 7069–7073.
- (16) Wu, H. *Phys. Rev. B* **2010**, *82*, 020410(R).
- (17) Fuwa, Y.; Wakeshima, M.; Hinatsu, Y. *Solid State Commun.* **2010**, *150*, 1698–1701.
- (18) Ohoyama, K.; Kanouchi, T.; Nemoto, K.; Ohashi, M.; Kajitani, T.; Yamaguchi, Y. *Jpn. J. Appl. Phys.* **1998**, *37*, 3319–3326.
- (19) Rodríguez-Carvajal, J. *Physica B* **1993**, *192*, 55–69.
- (20) Blaha, P.; Schwarz, K.; Madsen, G. K. H.; Kvasnicka, D.; Luitz, J. *User's Guide for WIEN2k: An Augmented Plane Wave Plus Local Orbitals Program for Calculating Crystal Properties*; Vienna University of Technology: Vienna, 2001; ISBN 3-9501031-1-2.
- (21) Wills, A. S. *Physica B* **2000**, *276–278*, 680–681.
- (22) Matoba, M.; Takeuchi, T.; Okada, S.; Kamihara, Y.; Itoh, M.; Ohoyama, K.; Yamaguchi, Y. *Physica B* **2002**, *312–313*, 630–631.

JA109007G